

Electronic Supplementary Information

Dual-emission MOF-dye sensor for ratiometric fluorescence recognition of RDX and detection of a broad class of nitro-compounds

Hong-Ru Fu,^a Li-Bing Yan,^a Nai-Teng Wu,^a Lu-Fang Ma,^{*a,b} Shuang-Quan Zang^{*,b}

^a College of Chemistry and Chemical Engineering, Henan Province Function-oriented Porous Materials Key Laboratory, Luoyang, Normal University, Luoyang 471934, P. R. China

^b College of Chemistry and Molecular Engineering, Zhengzhou University, Zhengzhou, 450001 Henan, P. R. China.

** Corresponding Author*
E-mail: mazhuxp@126.com
E-mail: zangsqzg@zzu.edu.cn

Contents

- 1. General methods.**
- 2. The encapsulation of dye**
- 3. The luminescent emission of 1-HPTS in the common solvents.**
- 4. Thermogravimetric Analysis of MOFs**
- 5. The sensing of the nitro-containing compounds in aqueous solution**
- 6. The calculations of the HOMOs and LUMOs of the nitro-explosives**
- 7. The UV-vis spectra**
- 8. Powder X-ray Diffraction Studies**

1. General methods.

All reagents and solvents used in this work were commercially available. 8-hydroxy-1,3,6-Pyrenetrisulfonic acid were purchased from Alfa. The tris(4-(1H-imidazol-1-yl)phenyl)amine (TIPA) ligand was prepared by literature methods.¹ Deionized water was used as solvent in this work. Powder X-ray diffraction analysis has been determined on a D/Max-2500 X-ray diffractometer using Cu-K α radiation. C, H, and N microanalyses were carried out with a PerkinElmer 240 elemental analyzer. Thermal analysis were measured by the NETSCHZ STA-449C thermoanalyzer with a heating rate of 5 °C/min under an air atmosphere. Ultraviolet-visible (UV-vis) adsorption spectra were collected on a PerkinElmer Lambda 35 spectrophotometer. The luminescent measurements were performed on a Hitachi F-7000 Fluorescence spectrophotometer.

2. The encapsulation of dye

The anion exchange capacity of compound **1** were evaluated by measuring the decolorization rate of aqueous HPTS solution, which was calculated by the following formula:

$$q_e = \frac{(C_i - C_e)V}{W}$$

where C_i and C_e (mg g⁻¹) are the initial and equilibrium HPTS concentration, respectively. V (mL) is the volume of HPTS solution, W (mg) is the mass of adsorbent. After exchange, the solid samples were centrifuged, rinsed with water and dried in the air, namely **1**⊃HPTS.

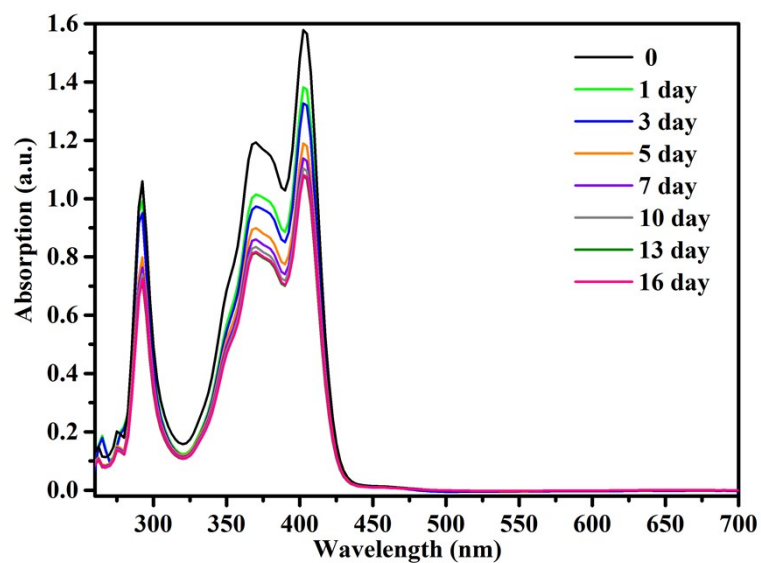


Figure S1. UV-vis absorption spectra of HPTS exchange solution, the exchange process was carried out in 5×10^{-3} mol L⁻¹ aqueous solution of HPTS.

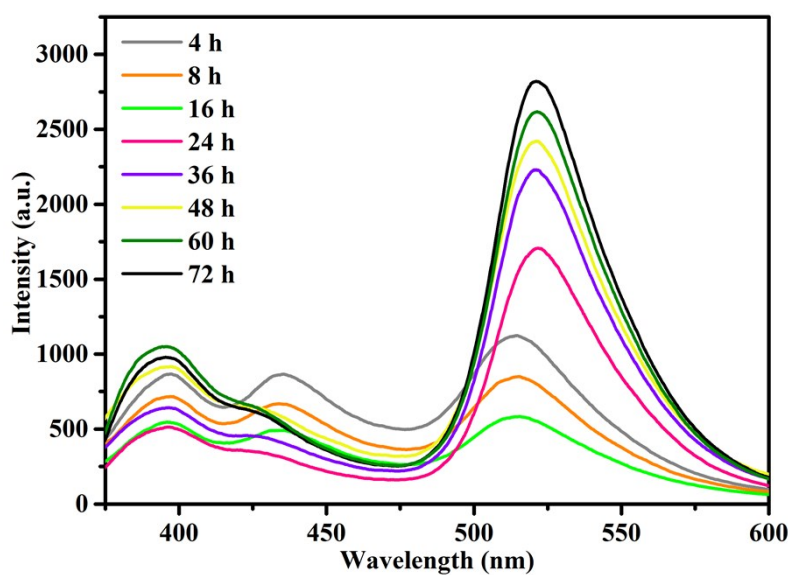


Figure S2. The change of fluorescence intensity of the dual signals during the ion-exchange process.

3. The luminescent emission of 1>HPTS in the common solvents.

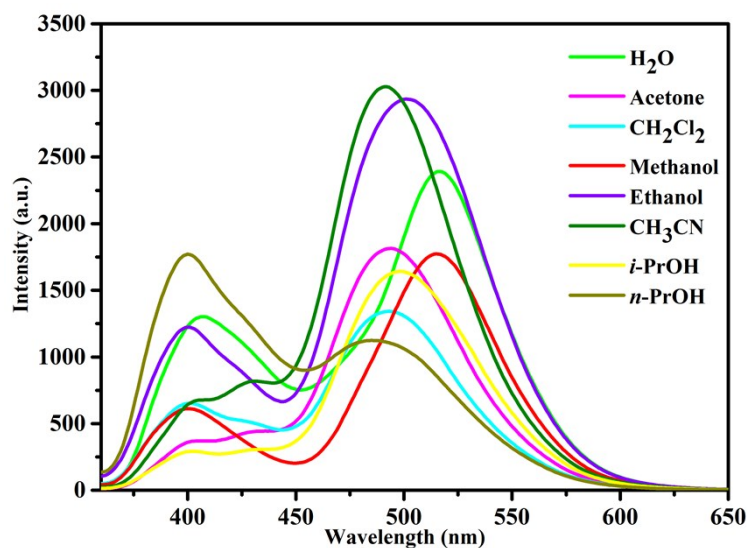


Figure S3. The luminescence emission of 1>HPTS in the common solvents.

4. Thermogravimetric Analysis of MOFs

Thermal Gravimetric Analysis (TGA) was carried out using a NETSCHZ STA-449C simultaneous TG thermoanalyzer, under the air atmosphere (flow rate 20 mL min⁻¹) over the temperature range of 30 to 800 °C and at a heating rate of 5 °C min⁻¹.

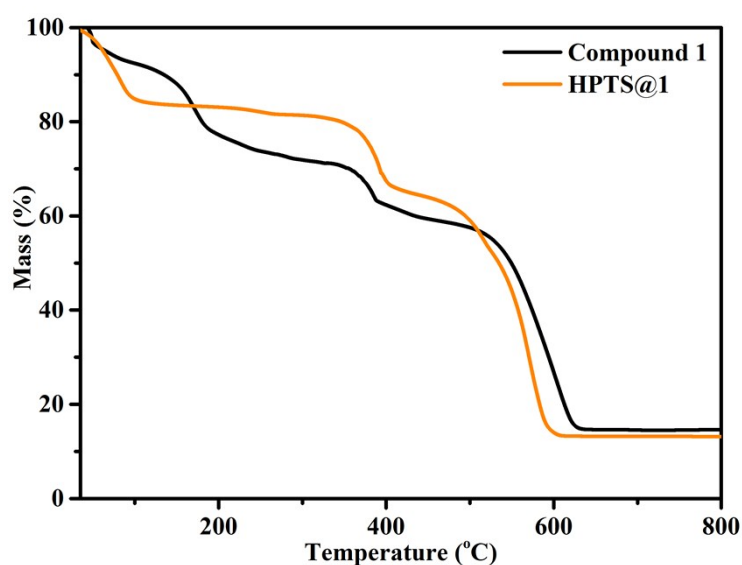


Figure S4. TGA curves of compound 1 and 1>HPTS under air atmosphere.

5. The sensing of the nitro-containing compounds in aqueous solution

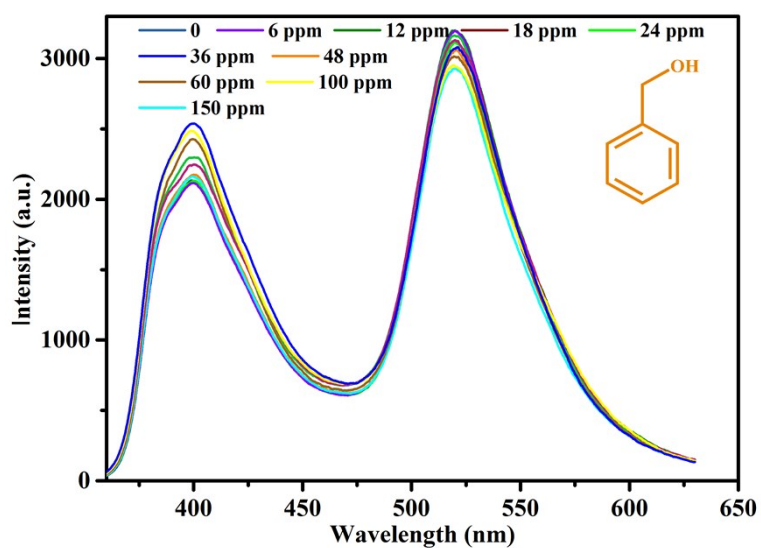


Figure S5. The change in fluorescence intensity of 1-HPTS with gradual increment of phenethyl alcohol in aqueous solution.

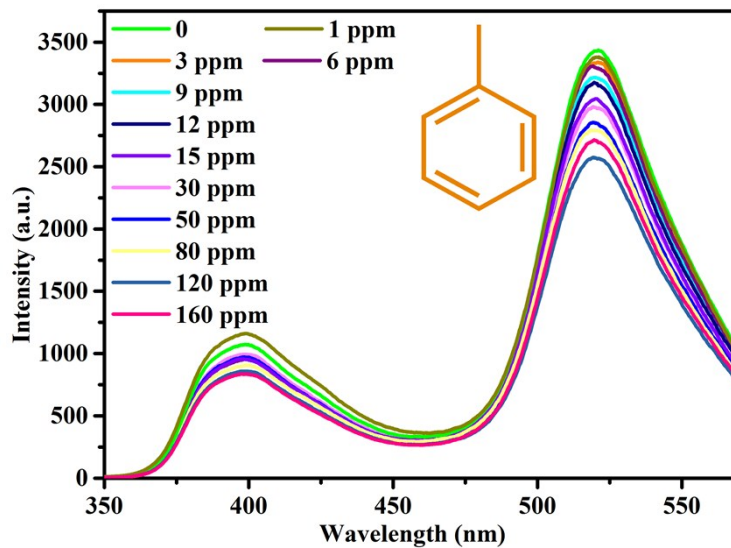


Figure S6. The change in fluorescence intensity of 1-HPTS with gradual addition of toluene in aqueous solution.

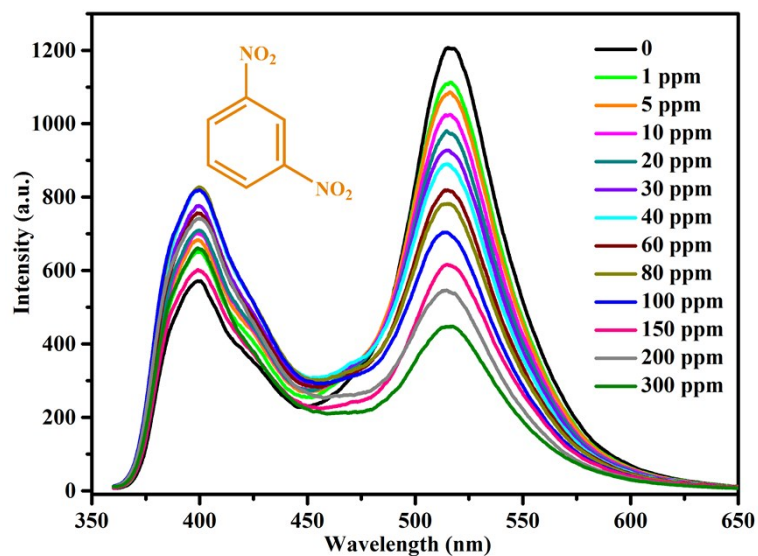


Figure S7. The change in fluorescence intensity of **1-HPTS** with gradual addition of 1,3-DNB in aqueous solution.

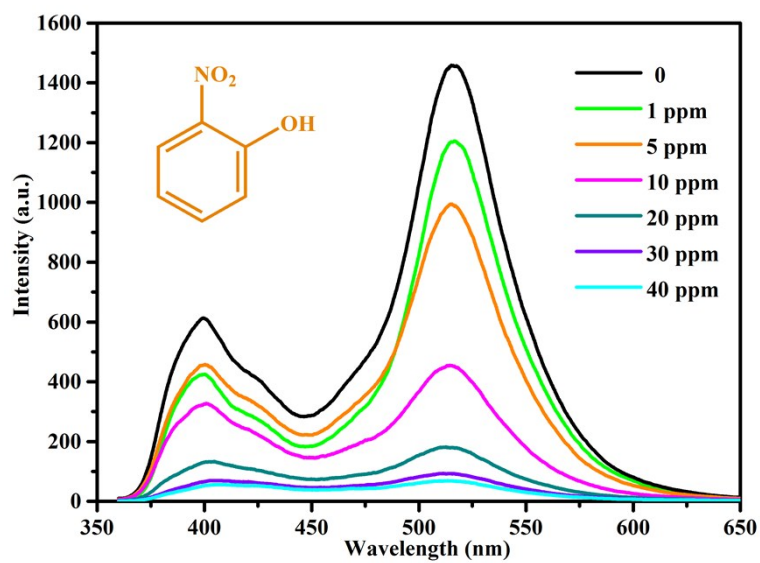


Figure S8. The change in fluorescence intensity of **1-HPTS** with gradual addition of 2-NP in aqueous solution.

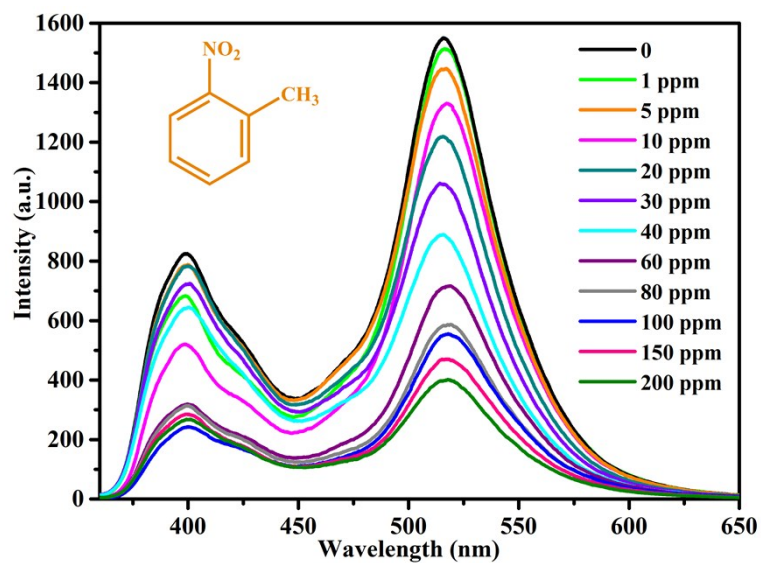


Figure S9. The change in fluorescence intensity of 1-HPTS with gradual addition of 2-NT in aqueous solution.

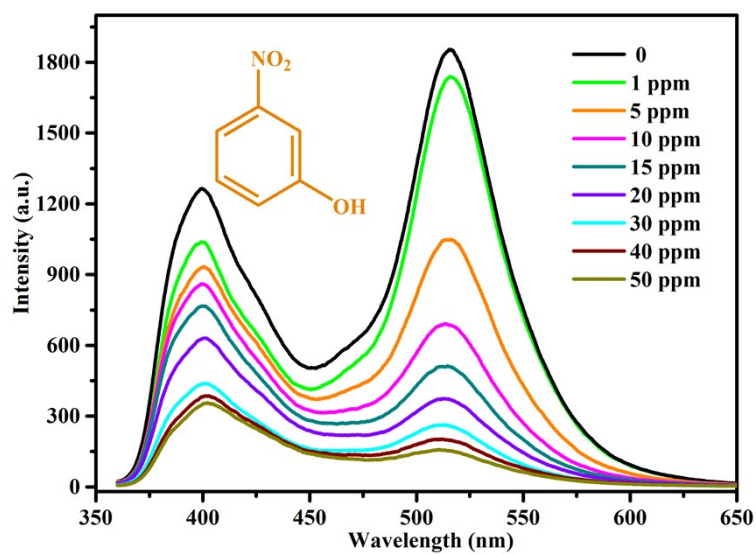


Figure S10. The change in fluorescence intensity of 1-HPTS with gradual addition of 3-NP in aqueous solution.

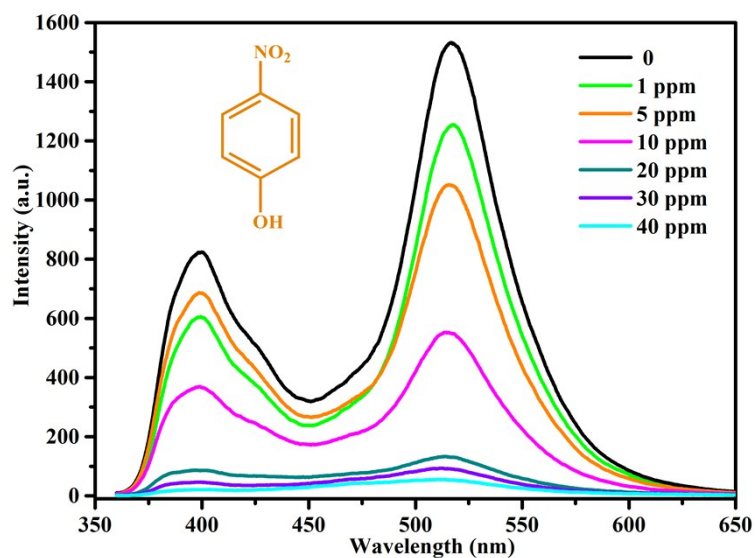


Figure S11. The change in fluorescence intensity of 1DHPST with gradual addition of 4-NP in aqueous solution.

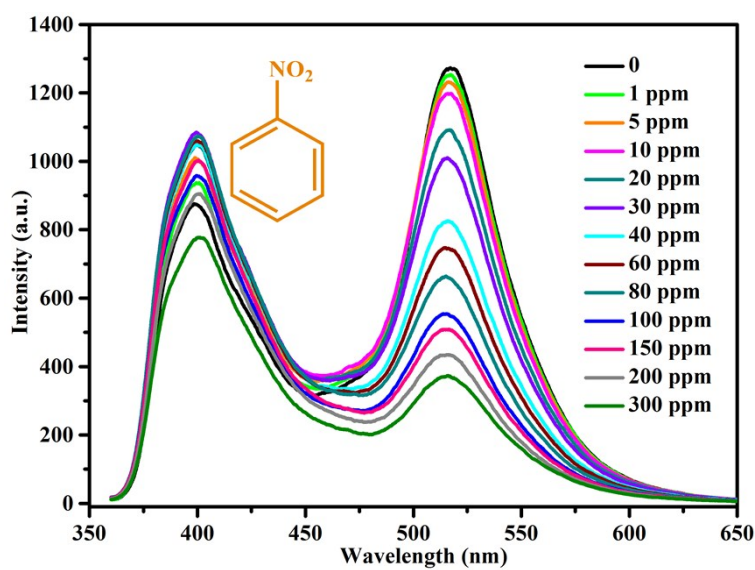


Figure S12. The change in fluorescence intensity of 1DHPST with gradual addition of NB in aqueous solution.

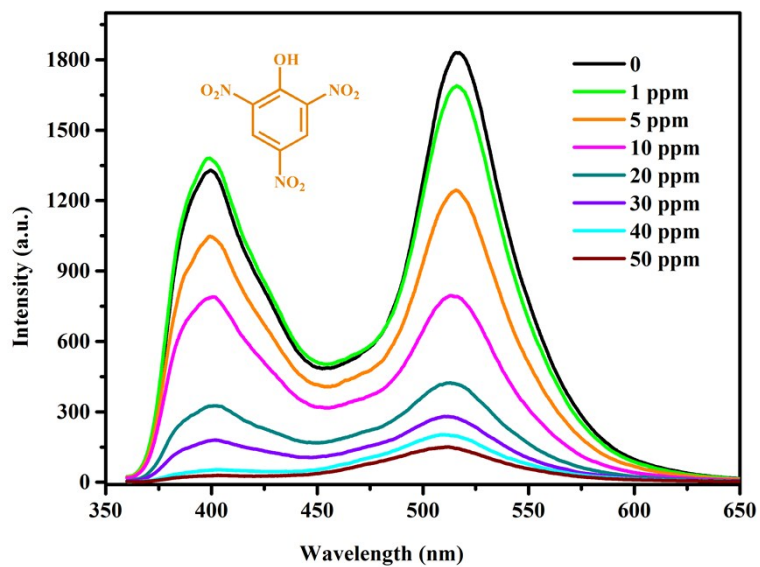


Figure S13. The change in fluorescence intensity of 1-HPTS with gradual addition of TNP in aqueous solution.

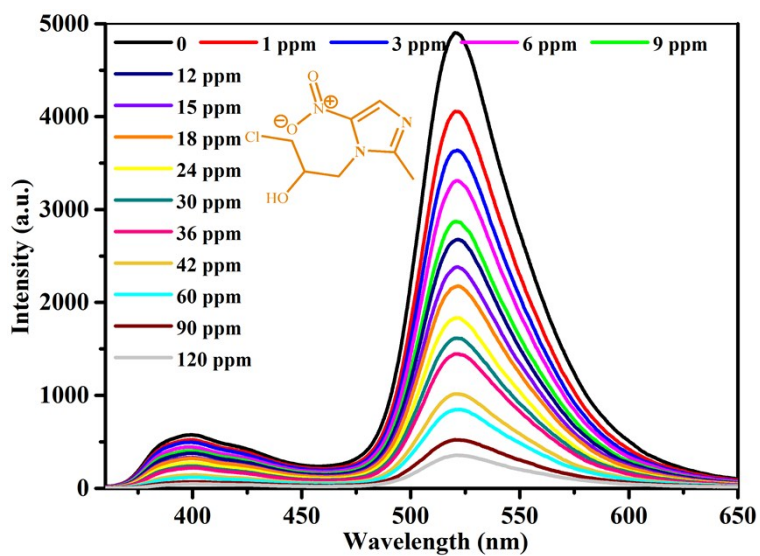


Figure S14. Fluorescence emission profile 1-HPTS towards ODZ through the gradual addition of ODZ aqueous solution .

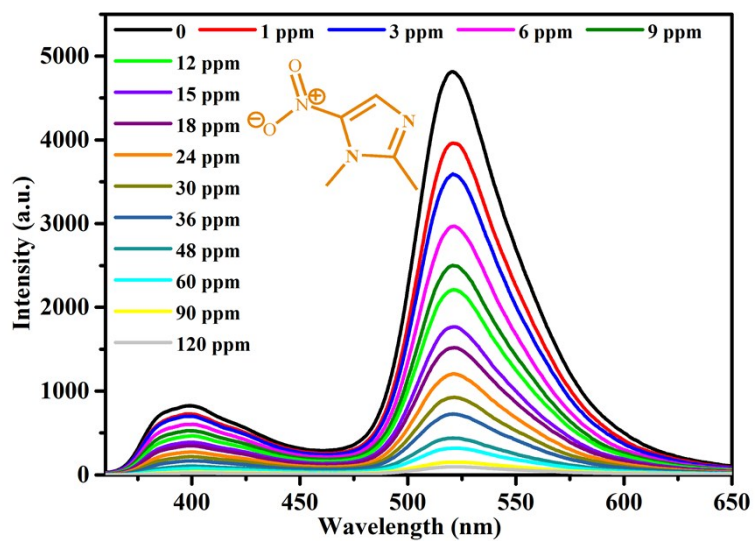


Figure S15. Fluorescence emission profile 1-HPTS towards DTZ through the gradual addition of DTZ aqueous solution.

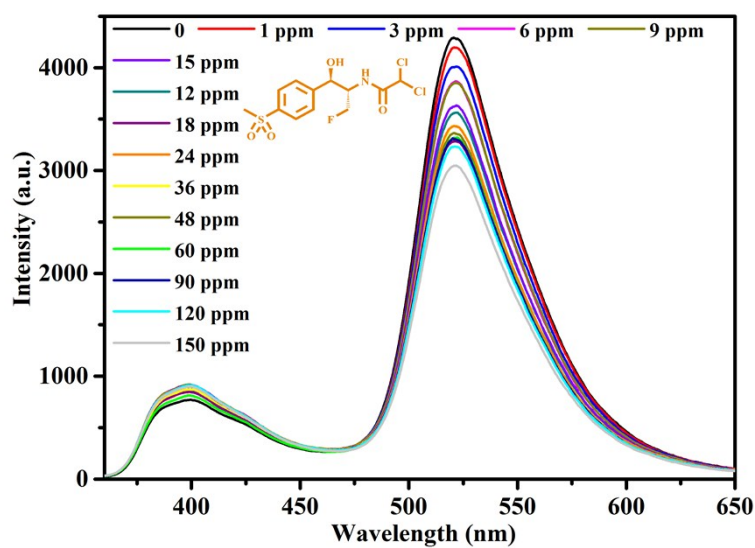


Figure S16. Fluorescence emission profile 1-HPTS towards FFC through the gradual addition of FFC aqueous solution.

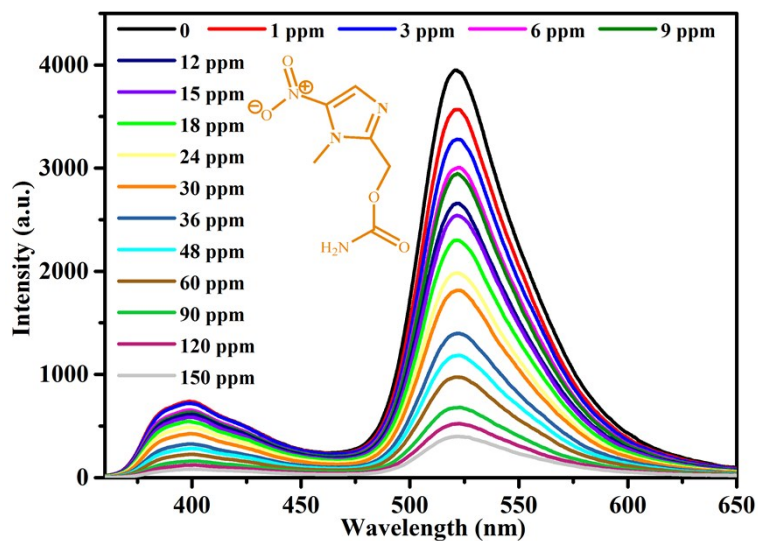


Figure S17. Fluorescence emission profile **1-HPTS** towards MDZ through the gradual addition of MDZ aqueous solution.

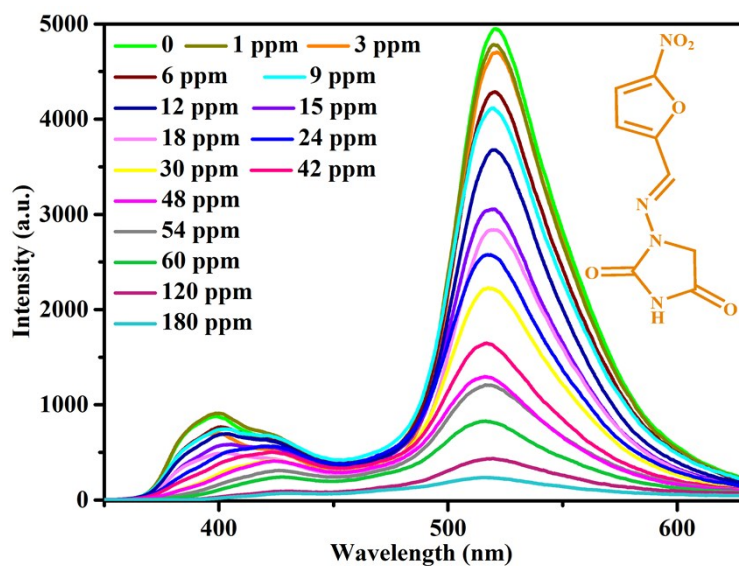


Figure S18. Fluorescence emission profile **1-HPTS** towards NFT through the gradual addition of NFT aqueous solution.

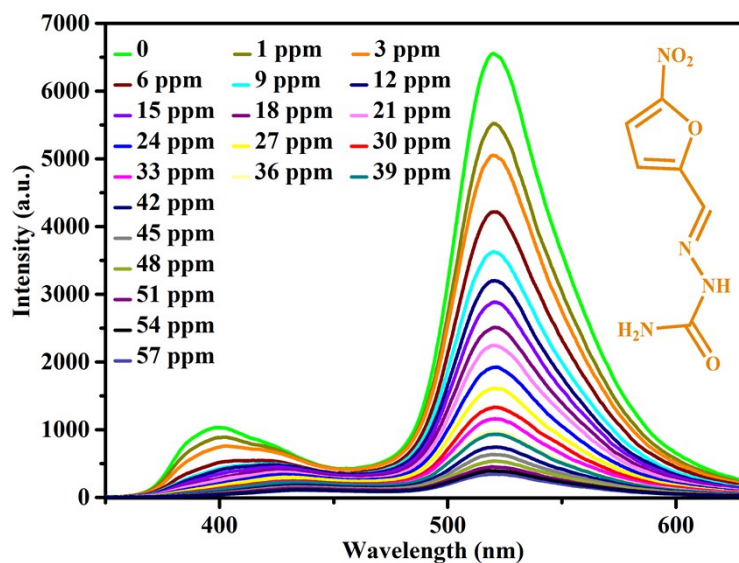


Figure S19. Fluorescence emission profile 1-HPTS towards NZF through the gradual addition of NZF aqueous solution.

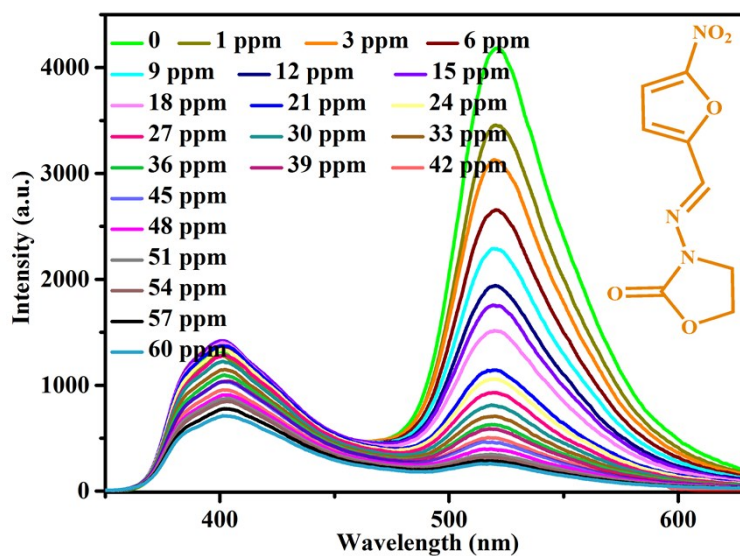


Figure S20. Fluorescence emission profile 1-HPTS towards FZD through the gradual addition of FZD aqueous solution.

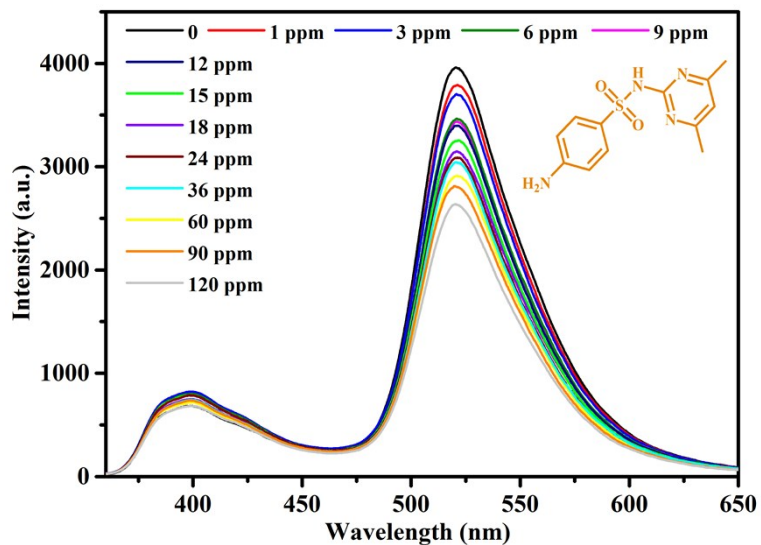


Figure S21. Fluorescence emission profile 1-HPTS towards SMZ through the gradual addition of SMZ aqueous solution.

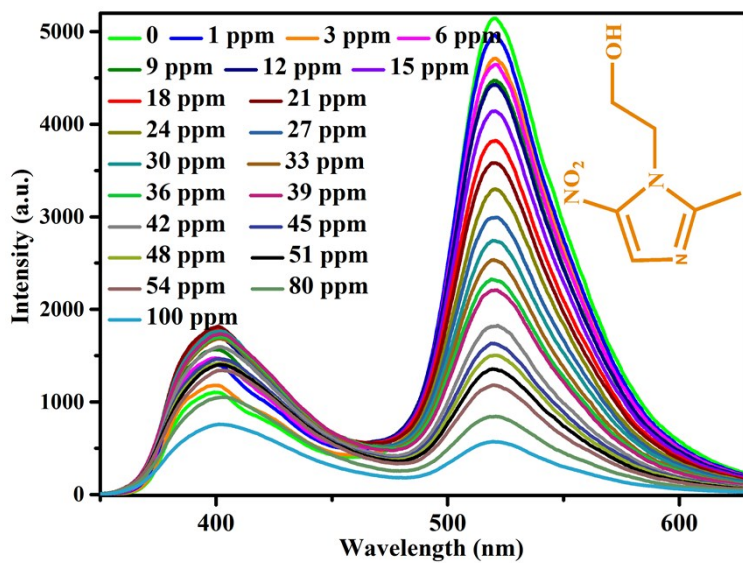


Figure S22. Fluorescence emission profile 1-HPTS towards MDZ through the gradual addition of MDZ aqueous solution.

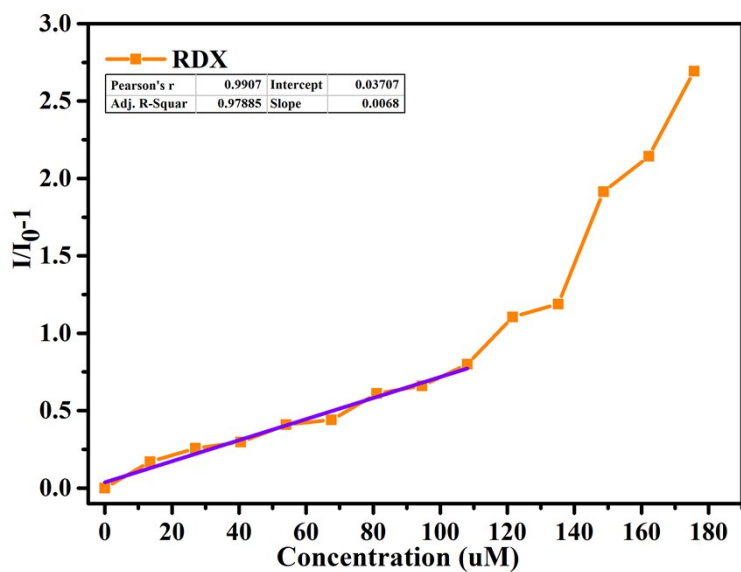


Figure S23. Corresponding Stern–Volmer plots of RDX, the purple line is linear fitting.

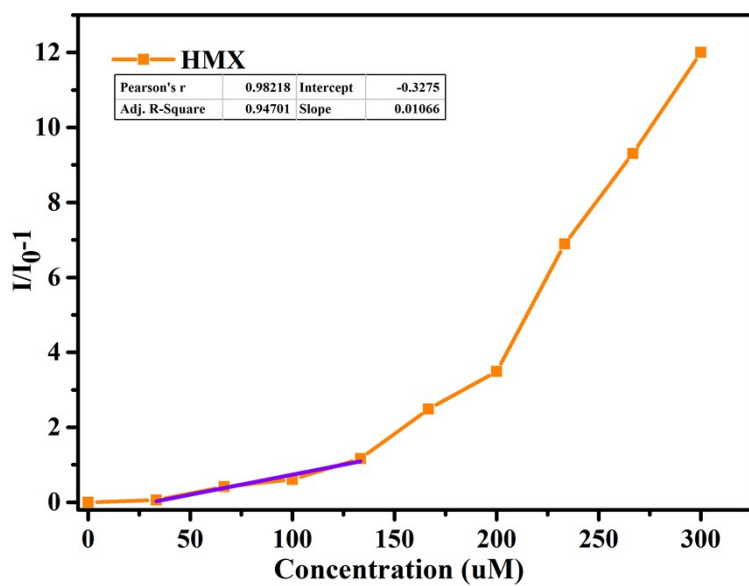


Figure S24. Corresponding Stern–Volmer plots of HMX, the purple line is linear fitting.

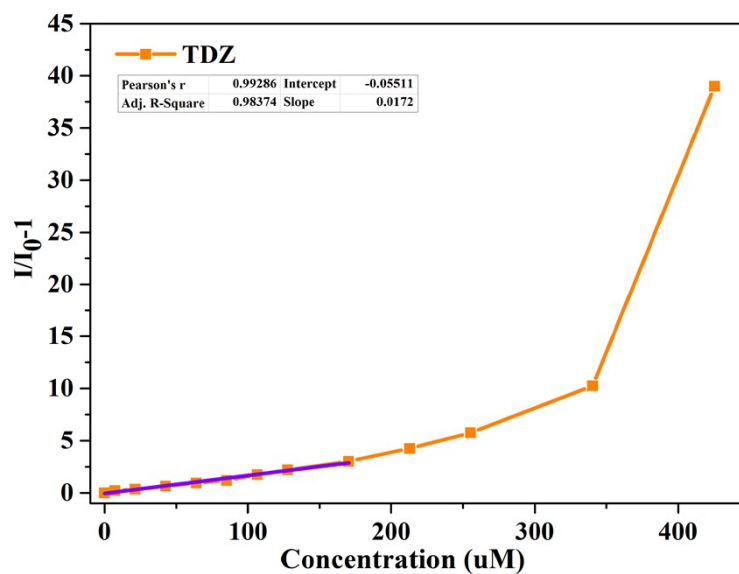


Figure S25. Corresponding Stern–Volmer plots of DTZ, the purple line is linear fitting.

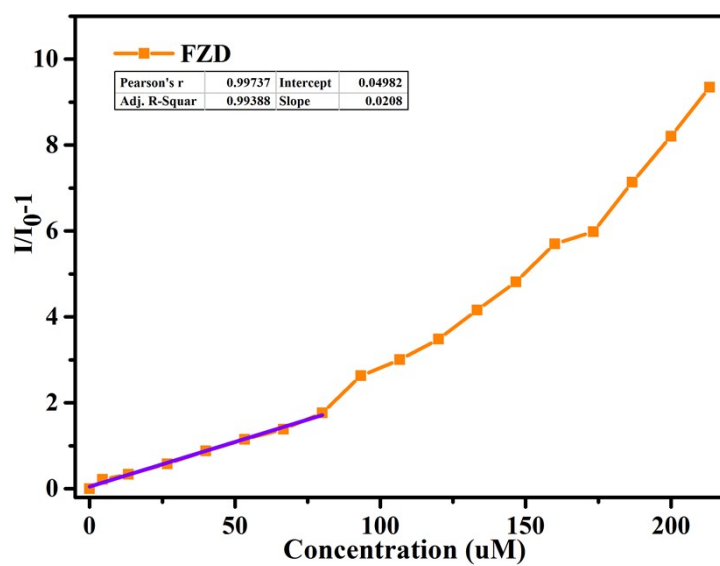


Figure S26. Corresponding Stern–Volmer plots of FZD, the purple line is linear fitting.

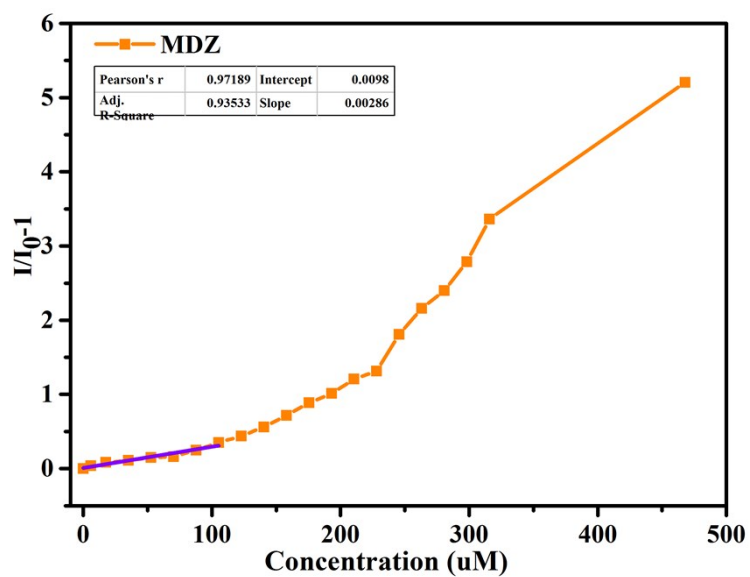


Figure S27. Corresponding Stern–Volmer plots of MDZ, the purple line is linear fitting.

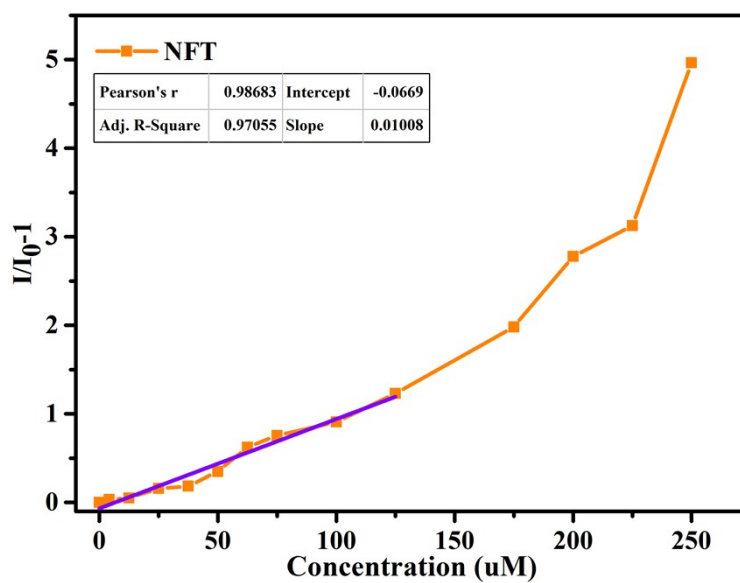


Figure S28. Corresponding Stern–Volmer plots of NFT, the purple line is linear fitting.

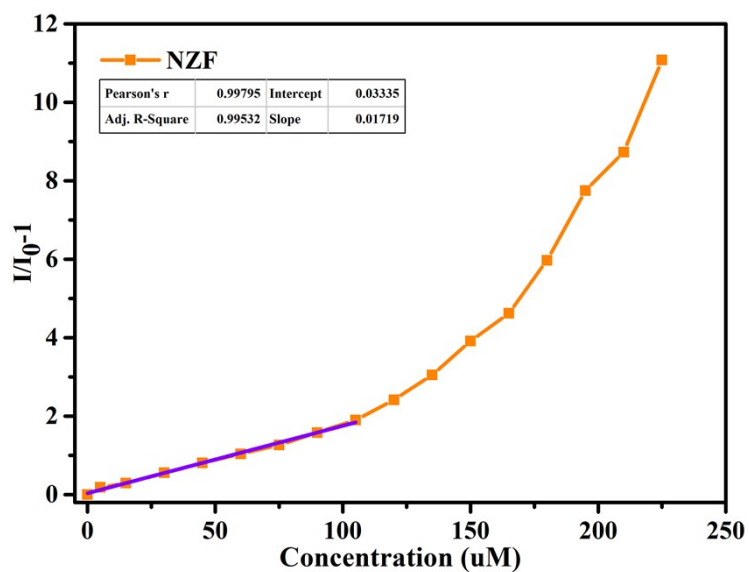


Figure S29. Corresponding Stern–Volmer plots of NZF, the purple line is linear fitting.

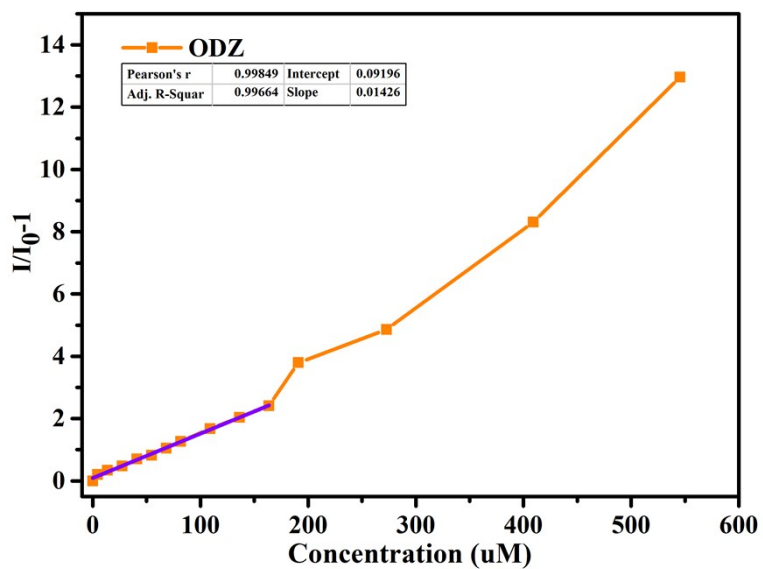


Figure S30. Corresponding Stern–Volmer plots of ODZ, the purple line is linear fitting.

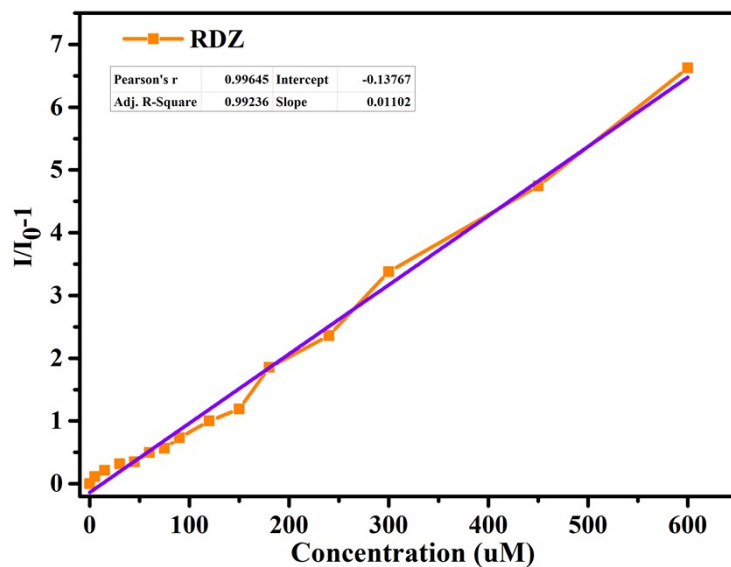


Figure S31. Corresponding Stern–Volmer plots of RDZ, the purple line is linear fitting.

6. The calculations of the HOMOs and LUMOs of the nitro-explosives

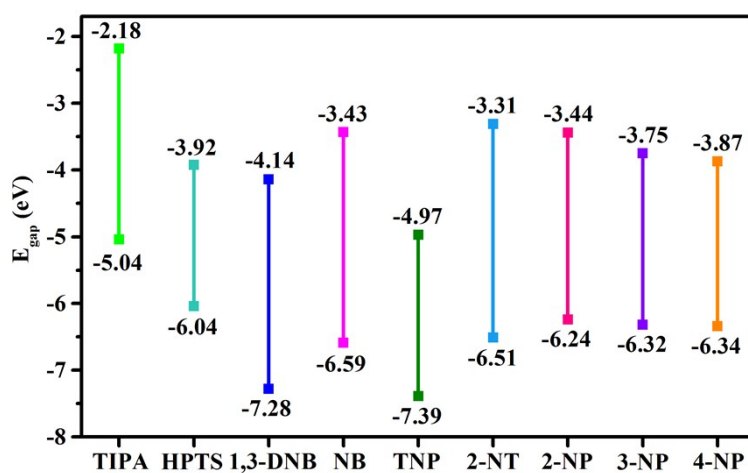


Figure S32. The calculations of the HOMOs and LUMOs of the nitro-explosives.

7. The UV-vis spectera

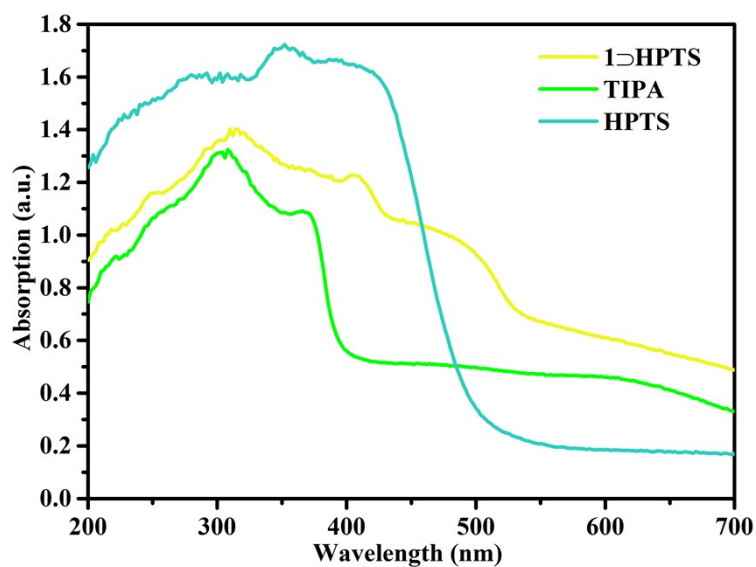


Figure S33. UV-vis absorption spectrum of compound **1**, TIPA and **1D**-HPTS in solid state.

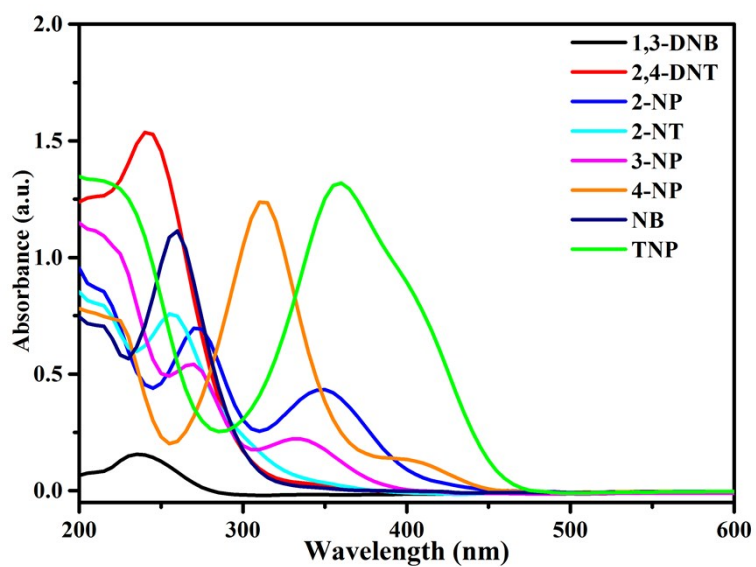


Figure S34. UV-vis absorption spectrum of nitro explosives in aqueous solution.

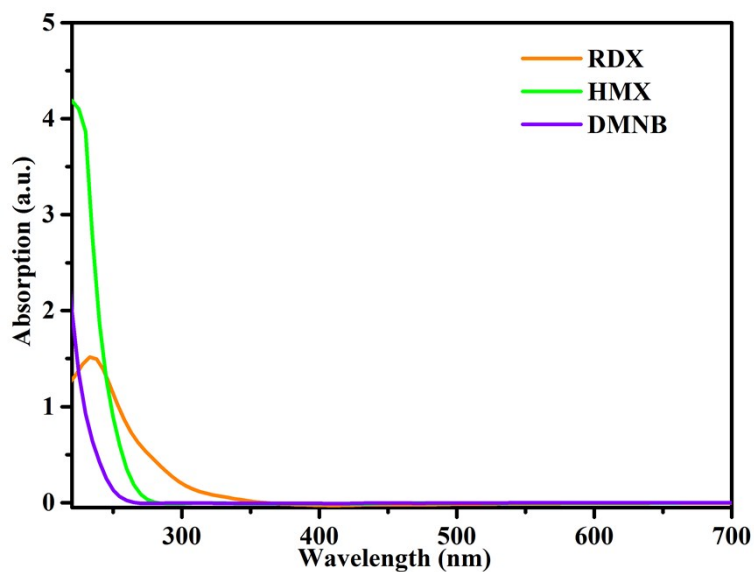


Figure S35. UV-vis absorption spectrum of aliphatic nitro-organics in aqueous solution.

8. Powder X-ray Diffraction Studies

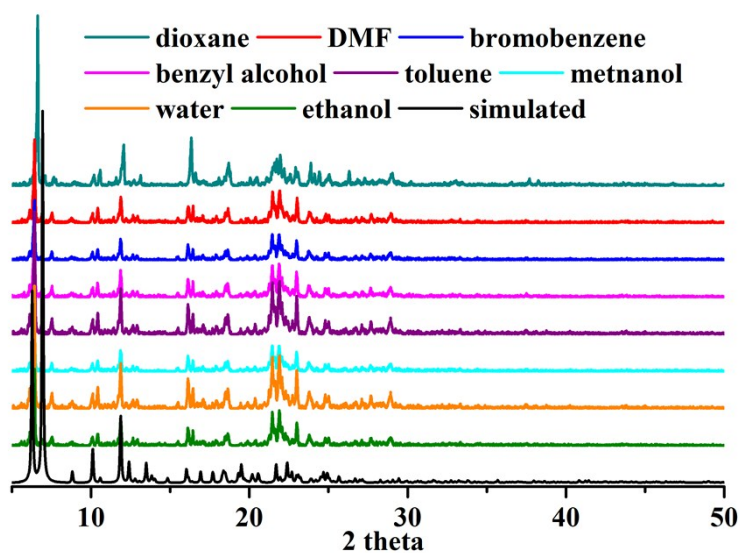


Figure S36. PXRD patterns of 1D-HPTS after being submerged in the various solvents for one days, except in water, methanol and ethanol for two weeks.

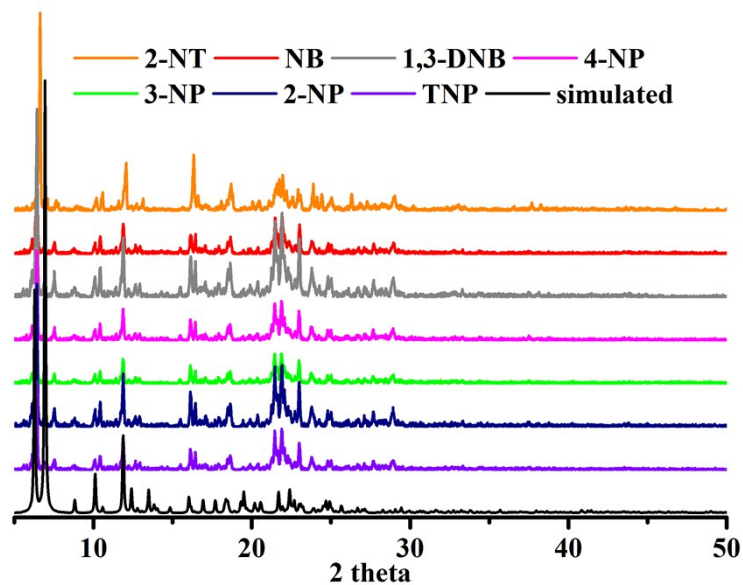


Figure S37. PXRD patterns of 1D-HPTS after fluorescence titration in the aqueous solutions of the various nitro explosives (the concentration of each species is 300 ppm).

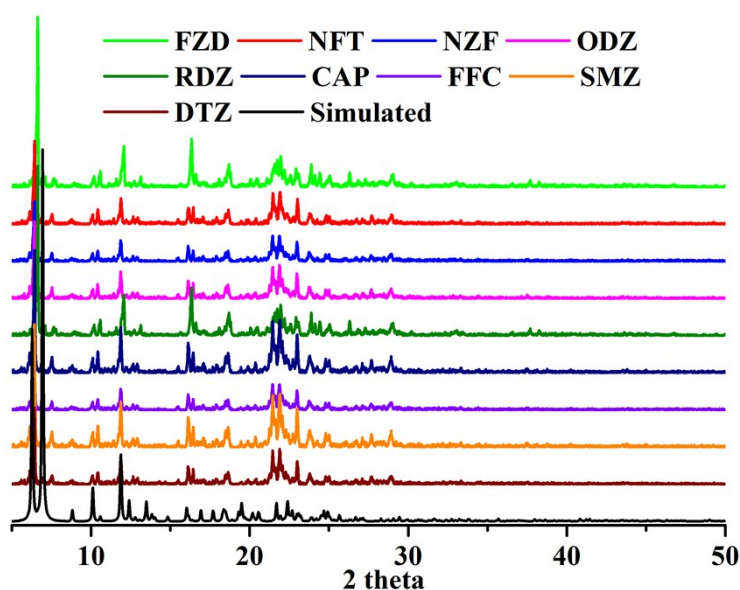


Figure S38. PXRD patterns of 1D-HPTS after fluorescence titration in the aqueous solutions of the various nitro-containing antibiotics (the concentration of each species is 200 ppm).

References

1. H. R. Fu, Z. X. Xu, J. Zhang, *Chem. Mater.*, 2015, **27**, 205–210.